Geomechanics and Engineering, *Vol. 25, No. 2 (2021) 111-121*
DOI: https://doi.org/10.12989/gae.2021.25.2.111

Investigation of blasting impact on limestone of varying quality using FEA

Lamprini S. Dimitraki*[1], Basile G. Christaras[1a] and Nikolas D. Arampelos[2b]

[1]*School of Geology, Faculty of Sciences, Aristotle University of Thessaloniki, Thessaloniki, Greece*
[2]*School of Civil Engineering, Aristotle University of Thessaloniki, Thessaloniki, Greece*

(Received January 7, 2021, Revised March 22, 2021, Accepted March 29, 2021)

Abstract. Large deformation and rapid pressure propagation take place inside the rock mass under the dynamic loads caused by the explosives, on quarry faces in order to extract aggregate material. The complexity of the science of rock blasting is due to a number of factors that affect the phenomenon. However, blasting engineering computations could be facilitated by innovative software algorithms in order to determine the results of the violent explosion, since field experiments are particularly difficult to be conducted. The present research focuses on the design of a Finite Element Analysis (FEA) code, for investigating in detail the behavior of limestone under the blasting effect of Ammonium Nitrate & Fuel Oil (ANFO). Specifically, the manuscript presents the FEA models and the relevant transient analysis results, simulating the blasting process for three types of limestone, ranging from poor to very good quality. The Finite Element code was developed by applying the Jones-Wilkins-Lee (JWL) equation of state to describe the thermodynamic state of ANFO and the pressure dependent Drucker-Prager failure criterion to define the limestone plasticity behavior, under blasting induced, high rate stress. A progressive damage model was also used in order to define the stiffness degradation and destruction of the material. This paper performs a comparative analysis and quantifies the phenomena regarding pressure, stress distribution and energy balance, for three types of limestone. The ultimate goal of this research is to provide an answer for a number of scientific questions, considering various phenomena taking place during the explosion event, using advanced computational tools.

Keywords: rock blasting; limestone; ANFO; finite element analysis; quarry

1. Introduction

The implementation of the blasting process on quarry faces is a widespread practice in the mining industry. The explosives, such as Ammonium Nitrate (94%) & Fuel Oil (6%) (ANFO), are the main source of concentrating chemical energy for rock fragmentation and extraction of aggregate. The performance of the explosives and the monitoring of the effects inside the rock mass, constitute an attractive subject for investigation, throughout the decades, by the scientific community such as, Clark (1987), Mohanty (1996), Rosa and Thornton (2011), Singh *et al.* (2016), Ozacar (2018), Song *et al.* (2018).

Based on several references, (Kuznetsov 1973, Rustan *et al.* 1983, Lilly 1986, Stagg *et al.* 1992, Scott *et al.* 1993, Franklin and Maerz 1996, Liu *et al.* 2019, Dimitraki *et al.* 2019), there are many geotechnical factors that affect the blastability of the rock mass, intensifying the complexity of the problem. These factors include the properties of the intact rock such as strength, elastic-plastic range and density, as well as the characteristics of the discontinuities such as orientation and distance that define the volume of the blocks in-situ. The initial properties of the rock mass are undergone severe changes due to blasting impact, affecting the behavior such as stress distribution, strength and deformability (Kwon *et al.* 2009). Furthermore, factors of utmost importance are the nature of the explosive material, the thermodynamic state, the geometry of the pit face and the blast hole pattern. Additionally, the rock mass fragmentation depends on its density, defining the propagation of the energy inside the rock mass. It is well known that shock waves are generated inside the rock mass during the explosion, with stress often exceeding the compressive strength of the rock, creating fracture formation around the blast hole. The shock waves travel in the rock mass until they are reflected on free faces or pre-existed discontinuities, returning as tensile waves. The gas pressure, which is generated from the decomposition of the explosive material, also plays an important role in the fracture mechanism. A volume of high pressured gas causes radial fractures which finally lead to the spalling of the blocks, (Nie and Olsson 2000).

It is clear that conducting field experiments, for studying the blasting phenomenon inside the rock mass, is a costly, very complicated and oftentimes not feasible process. However, numerical analysis methods, such as Finite Element Analysis (FEA), offer the capability to simulate the blasting event on the pit face in relation to time and space, investigating analytically the process of the explosion and the conditions that are developed inside the rock mass. Specifically, numerical simulation is widely used as a common practice for solving extremely complex problems

*Corresponding author, Postdoctoral Researcher
E-mail: ldimitr@geo.auth.gr
[a]Professor
E-mail: christar@geo.auth.gr
[b]M.Eng., Civil Engineer
E-mail: arampelosn@gmail.com

ISSN: 2005-307X (Print), 2092-6219 (Online)

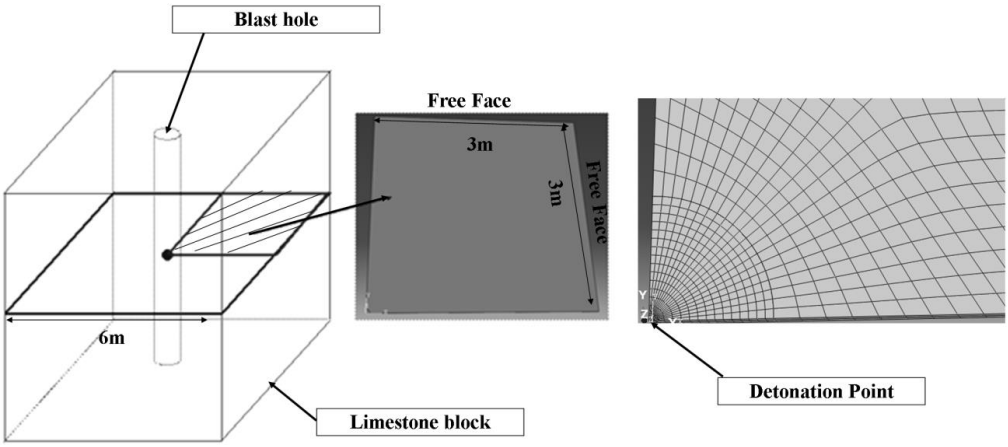

Fig. 1 Geometry and FEA mesh for the simulated single blast hole model

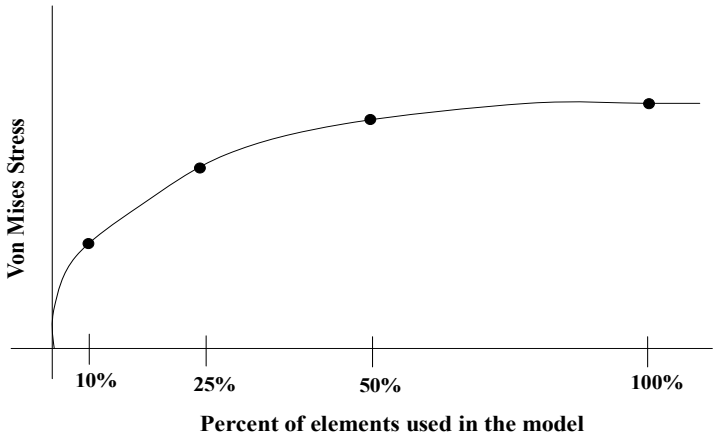

Fig. 2 Convergence plot for the determination of the mesh density

that are described by complicated geometry, thermodynamic states and boundary conditions. This process is a constantly evolving numerical method which can be used to simulate a continuous medium, such as the pit face.

By applying the above principles, the present study focuses on simulating the conditions near a blast hole, inside a limestone pit face, taking into consideration not only the geometric characteristics of the face and the features of the explosive material of ANFO, but also the quality of the limestone. In this paper, three types of limestone of different quality were simulated, depending on the mechanical and stress-strain characteristics of each type. The three types of limestone are designated as of Very Good Quality (VGQ), Good Quality (GQ) and Poor Quality (PQ).

In literature there are a number of references to the numerical simulation of the blasting load (Yang *et al.* 1996, Golshani *et al.* 2007, Ma and An 2008, Zhou 2010, Sazid and Singh 2012, Zhang *et al.* 2018). However, information on the comparative behavior of different qualities of limestone during the blast performance is scarce. Therefore the authors' approach attempts to cover this deficiency, by comparing the response of different qualities of limestone under blasting. Specifically, the current research presents results that describe the influence of the mechanical characteristics of the limestone on pressure wave propagation, energy balance and stress wave propagation, verifying some well-known physical phenomena. Finally, it should be mentioned that the present analysis is a precursor of a future research which will be conducted with different structures of the limestone taking into consideration joints characteristics.

2. Numerical modeling description

2.1 Finite element model

The numerical simulation was performed using the explicit finite element method, which offers the capability to analyze high rate, short duration, dynamic problems, such as explosions. The explicit method requires many small time steps and the stability limit for the largest time increment is closely related to the time required for a stress wave to cross the smallest element dimension. The present model simulates a limestone block with dimensions of 6.00 m x 6.00 m and a single blast hole of 0.05 m radius, using biaxial symmetry for reducing computational time. Specifically, the model includes the one fourth part of the square, in medium depth of the entire rock mass block, with a negligible thickness. Aside from the two forming free faces, suitable boundary restraints were implemented on all

remaining faces, using symmetry displacement conditions (the displacement vector component perpendicular to the plane is zero and the rotational vector components parallel to the plane are zero). The model's mesh consists of hexahedron-shaped solid elements, Fig. 1. After many attempts, the final mesh was achieved with an increasing number of elements until convergence was achieved, according to the relevant plot Fig. 2. The convergence plot is a curve of a critical result parameter, which is typically some kind of stress, against the number of elements, (Abbey 2019). A number of convergence runs were performed to plot a curve which then was used to indicate the required convergence.

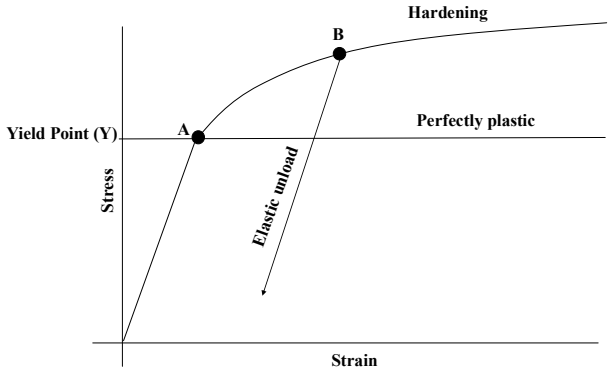

Fig. 3 Stress-strain curve with a typical hardening behavior

2.2 Rock mass behavior

Limestone behavior is closely related to the internal characteristics of the rock, such as mineral composition, structure, granular texture, porosity and density. However, in nature, it is also related to external conditions such as temperature, pressure and loading mechanism (Wei *et al.* 2018). Generally, limestone is characterized as a brittle material that behaves elastically until the point of yield, without presenting great potential for plastic deformation and with failure abruptly occurring at fracture. In the elastic deformation range, energy is not lost during the process of stressing and straining and strain is increased in a linear manner to the applied stress. The process of deformation is reversible as long as stress is kept under a certain value called yield stress. Exceeding this limit deformation is neither elastic nor fully reversible. Once yield occurs, then stress needs to be continually increasing to drive the plastic deformation. This natural process is called hardening and is represented in the stress-strain curve (Fig. 3) by a distinct upward trend. While loading past the yield point, the yield stress of the rock mass increases (from point A to point B). At this point if stress remains stable there will be no further strain, while if stress decreases, there will be elastic unloading leading to some remaining deformation. After a number of cycles of loading and elastic unloading, the yield stress of the rock will have further increased while the ductility of the material will have decreased significantly.

Another important behavioral aspect is the rock mass response to transient dynamic loading and its dependency on temporal features. The temporal features not only describe the effect of time on deformation and fracture, but also the temporal scales of the process related to the internal structure and physical-mechanical properties of the material, (Qi *et al.* 2016). The strain rate is an important feature of the rock mass behavior under dynamic loading and it can be described as the sensitivity of material strength to temporal deformation and fracture. It is noted that the effects on the material behavior for strain rates ranging from $1s^{-1}$ to$100s^{-1}$, are very important in high energy dynamic events such as blasting.

As far as modeling is concerned the rock mass is considered to be continuous and isotropic, without any joints or fractures. The elastic mechanical behavior can be designated by fundamental parameters like the elastic modulus and the Poisson's ratio, in order to predict the stress-strain performance under specific loading conditions. Moreover, the transition from the elastic to plastic range can be determined by various functions describing certain intensive conditions that lead to yield failure. These functions are often referred to as failure criteria. There is a number of failure criteria or yield criteria that correlate to stresses, strains, strain energy etc. The yield point is generally determined by the following expression (Potts and Zdravkovic 1999), Eq. (1).

$$F(\{\sigma\},\{\Upsilon\}) = 0 \tag{1}$$

where, $\{\sigma\}$ represents the intensive field and $\{\Upsilon\}$ the compressive or tensile strength of the material. When the yield function $F = 0$ the material yields, while when $F < 0$ the material presents linear behavior for the most part. The type of the function depends on specific characteristics of the material.

At the present paper, the Drucker-Prager failure criterion was implemented for defining the limestone plasticity under a blasting event, as an appropriate theory for pressure dependent, granular and frictional material, in conjunction with the Equation of State model to describe the dynamic response, estimating the stress state at which the rock reaches its ultimate strength, (Alejano and Bobet 2012). The Drucker-Prager failure criterion was also selected among others as a suitable theory, in which strain rate can be introduced as it affects the rock strength during the dynamic process. Also, this theory is suitable for materials such as limestone that present significantly greater compressive yield strength than tensile yield strength.

The Drucker-Prager criterion is a smooth approximation of the Mohr-Coulomb yield surface and a simple expansion of the Von Mises criterion and takes into consideration the hydrostatic stress for the calculation of the strength of the material. It can be expressed by the following equation, (Drucker and Prager 1952), Eq. (2).

$$\sqrt{J_2} = \lambda \acute{I}_1 + \kappa \tag{2}$$

where, $J_2 = \frac{1}{6}[(\sigma_1' - \sigma_2')^2 + (\sigma_1' - \sigma_3')^2 + (\sigma_3' - \sigma_1')^2]$ is the second invariant of the stress deviator tensor, $\acute{I}_1 = \sigma_1' + \sigma_2' + \sigma_3'$ is the first invariant of the stress tensor, λ and κ are material constants that depend on the friction and cohesion of the material, $\sigma_1', \sigma_2', \sigma_3'$ are the principle

effective stresses. Also, the Drucker-Prager yield surface is a function of pressure and the second invariant of the stress deviator tensor, Eq. (3):

$$f(p, J_2) = \sqrt{3J_2} - \beta \mathrm{p} - \mathrm{y} = 0 \quad (3)$$

where, $\mathrm{p} = -\frac{1}{3}(\sigma_1 + \sigma_2 + \sigma_3)$ is the pressure and y can be a function of plastic strain, plastic strain rate and temperature.

The yield surface is depicted as a cone surface in the principle stress space with its main axis coinciding with the hydrostatic one. Inside the cone no yield takes place while outside yielding occurs, Fig. 4.

There is a hardening rule which describes the evolution of the yield surface with plastic strain. The Drucker-Prager criterion, obeys to isotropic hardening. In this case, when the yield stress is exceeded, the yield surface expands proportionally in all directions. Specifically, beyond the yield point, after some cycles of loading and unloading, the material becomes harder and the elastic limit is higher both for tension and compression, Fig. 5. As far as the present research is concerned, the hardening behavior of the limestone, under the dynamic process, was defined by the yield stress in relation to the corresponding plastic strain also depending on the strain rate.

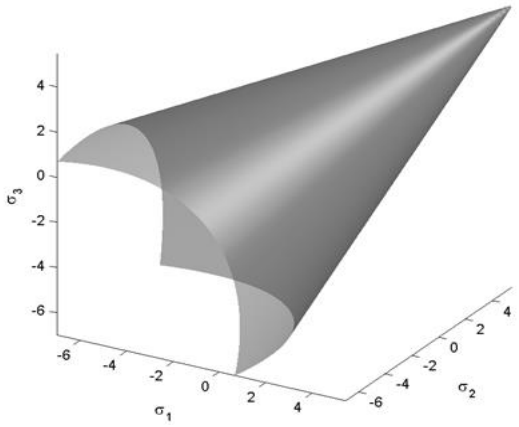

Fig. 4 Drucker-Prager yield surface in the principle stress space

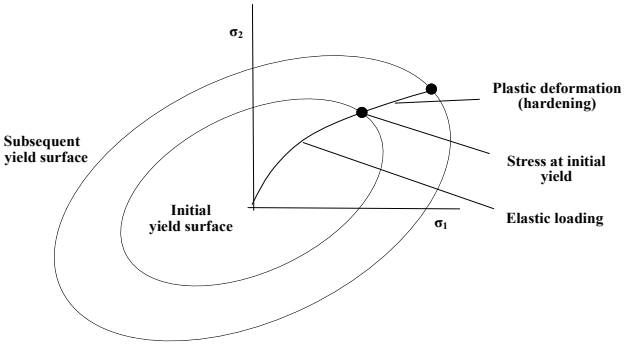

Fig. 5 Isotropic hardening

Table 1 Parameters for the three types of limestone that were used for the simulation

Parameter	Unit	VGQ	GQ	PQ
Density	t/m^3	2.70	2.65	2.58
Poisson's ratio	-	0.30	0.25	0.19
Young's Modulus	kPa	44E+06	36E+06	27E+06
Ultimate compressive stress	kPa	100E+03	82E+03	61E+03
Tensile Strength	kPa	10E+03	8200	6100

Moreover, the Drucker-Prager failure criterion was used in conjunction with a model of progressive damage and failure. The typical components of the progressive damage model are the damage initiation at the onset of the damage, the damage evolution law and finally the element removal from the mesh. Specifically, the damage initiation defines the point of initiation of stiffness degradation of the material, specifying the fracture plastic strain. Consequently, after damage initiation, the material stiffness is degraded progressively according to the specified damage evolution response. In particular, the damage evolution is an essential part of the damage formulation, which calculates the amount of the damage during the deformation process, according to the material behavior. At the current paper, the damage evolution law was determined with an associated parameter, the equivalent plastic displacement at failure. This parameter defines the damage as a function of the plastic displacement after damage initiation. Finally, the element removal option from the mesh was selected, once the material stiffness was fully degraded, leading to a complete loss of load carrying capacity.

Three types of limestone of different quality were simulated, depending on the mechanical and stress-strain characteristics of each type. The three types of limestone are designated as of Very Good Quality (VGQ), Good Quality (GQ) and Poor Quality (PQ). The parameters were defined based on literature by Wawersik and Fairhurst (1970), Stowe (1969), Christaras (1996) and Dimitraki *et al.* (2016). The relevant mechanical characteristics are presented in Table 1 and the stress-strain curves for each type are comparatively presented in Fig. 6. It should be noted that the tensile yield strength of limestone is much lower than the compressive yield strength by a factor of 10.

2.3 Explosive material and thermodynamic state

The Jones-Wilkins-Lee (JWL) Equation of State (EOS), which is used for modeling the thermodynamic state of the explosives in the current research, models the pressure, volume and energy relationship of the detonation products, generated by the release of chemical energy in an explosion. It has an empirical character that conforms to experiments and allows flexible calibration from experimental data at both early and large expansions (Souers *et al.* 1996, Hansson 2009). The pressure produced by the explosion is described by the JWL equation of state as shown in Eq. (4):

$$P = A\left(1 - \frac{\omega\rho}{R_1\rho_0}\right)e^{-R_1\frac{\rho_0}{\rho}} + B\left(1 - \frac{\omega\rho}{R_2\rho_o}\right)e^{-R2\frac{\rho_0}{\rho}} + \frac{\omega E\rho}{\rho_0} \quad (4)$$

where P is the pressure of the detonation products, ρ/ρ_o is the relative volume (i.e. the expansion ratio of the detonation products), A (kPa), B (kPa), R_1, R_2, ω are constants for each specific explosive, ρ_o and ρ the initial

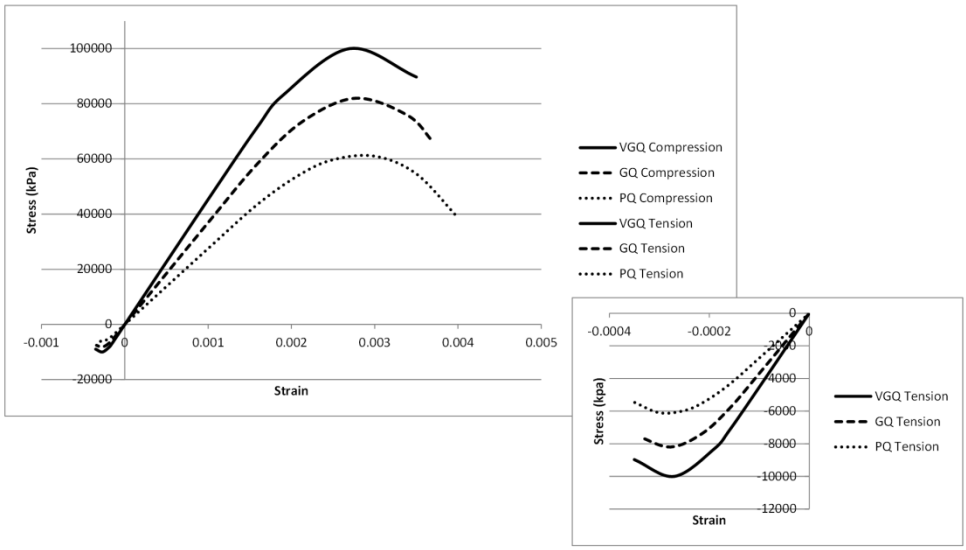

Fig. 6 Stress-strain curves for the three types of limestone based on literature

Table 2 ANFO properties and JWL EOS parameters

ANFO Properties			JWL EOS parameters				
Density (t/m^3)	Detonation wave speed (m/s)	Detonation Energy Density (kJ/t)	A (kPa)	B (kPa)	ω -	R_1 -	R_2 -
0.85	3200	3881000	266799000	3435000	0.39	7.037	1.159

and current density respectively, ω is a Grüneisen coefficient $\gamma - 1$, where γ is the adiabatic gamma for the detonation products at low pressure and E is the detonation energy density (kJ/t). Moreover, they are subjected to the constraints that $R_1 > R_2 > 0$ and $\omega > 0$, (Menikoff 2017). The JWL parameters can be determined either by numerical code or by the widely known cylinder test expansion measurements. At the current paper, the properties of explosive material of ANFO were used according to the experimental results of the cylinder test data by Sanchidrian *et al.* (2015). Table 2 presents the ANFO properties and JWL EOS parameters that were inserted into the model.

By taking into account the geometrical characteristics of the blast hole and the ANFO properties, the specific amount of energy of the explosive material is expected to be equal to $3881000 * \frac{3.14*0.05^2*0.01}{4} * 0.85 = 64.73$ kJ. This value actually is close enough to the result produced by the FEA and is depicted in Fig. 11.

3. Simulation results and discussion

3.1 Stress wave propagation

The explosion causes stresses that are characterized by a dynamic nature and the propagation of these stresses through the rock as a wave must be considered, (Jaeger *et al.* 2007). The stress waves include elastic waves, plastic waves and shock waves, according to the stress-strain relation of the material in which stress waves propagate.

Specifically, the stress waves that are generated inside the rock mass by blasting are generally elastic waves, except for the area close to the blast hole where the shock waves are generated, (Zhang 2016).

As far as the stress wave propagation inside the rock mass for the three qualities of limestone during the explosion is concerned, it is depicted in the following plot (Fig. 7), as it was produced by the numerical models. As it can be seen there is a rapid increase of the stress in a local area around the explosive center while smaller values are observed as the wave travels radially away from the blast hole. A ring of deleted elements is also observed around the blast hole, indicating the destruction of the rock mass and the maximum degradation of the stiffness. Furthermore, this plot demonstrates the difference of the wave propagation velocity and magnitude for the three types of limestone. It is obvious that the stress wave in the limestone that presents better quality characteristics is propagated faster than in the other two types. Comparatively, the stress wave in the VGQ limestone is propagated in 6.25E-04 s for a distance of 3.00 m, while in the GQ and PQ limestone the propagation presents latency for the same distance, 7.25E-04 s and 8.50E-04 s respectively. It is noted that after encountering the free faces, the stress waves create reflections on the boundaries, initiating rather complicated phenomena that are not discussed in the present paper.

3.2 Borehole pressure and stress wave pressure analysis

In the beginning of the blasting event, firstly a shock wave is formed and then the pressure wave follows in the reaction zone, which is a very thin zone behind the shock front of the blast hole. Immediately after the wave in the reaction zone follows the rarefaction wave. The composition of these three waves forms the detonation wave. The detonation wave acts as a shock wave causing an extremely high pressure on the wall of the borehole and then travels as ordinary stress wave in the region relatively

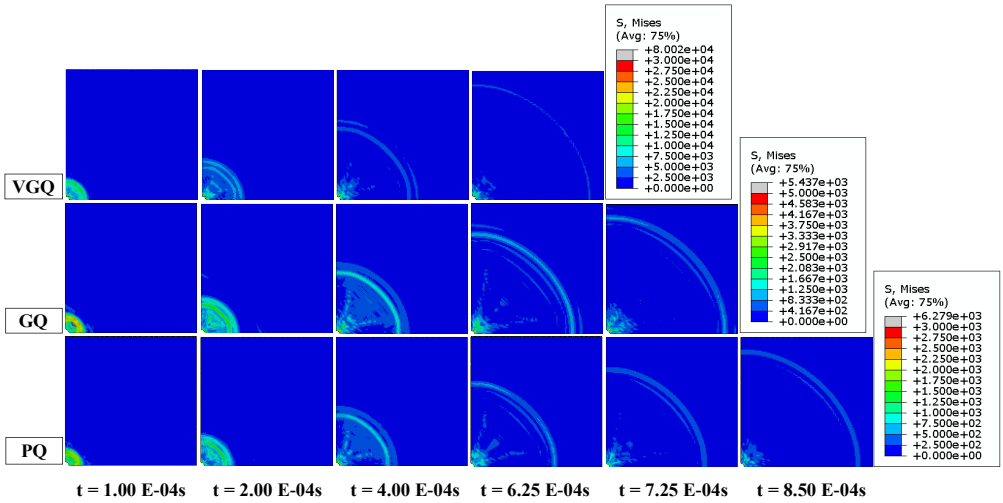

Fig. 7 Stress wave propagation over time for the three qualities of limestone

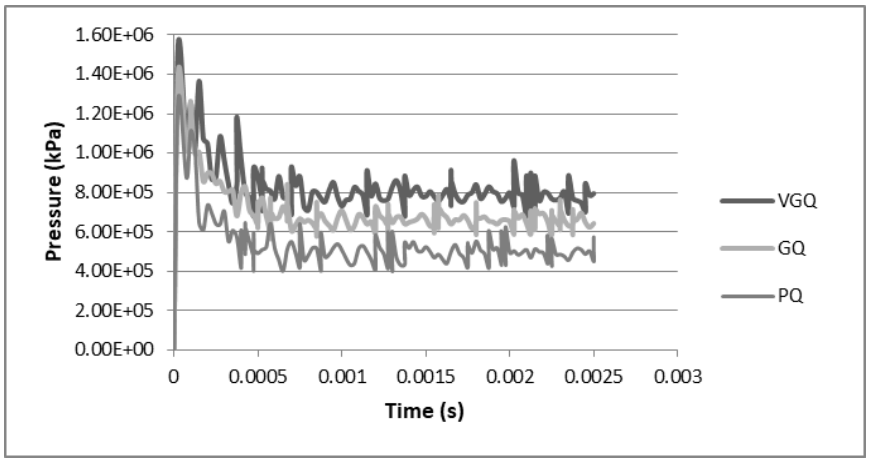

Fig. 8 Borehole pressure variation over time at the wall of the blast hole, for the three qualities of limestone

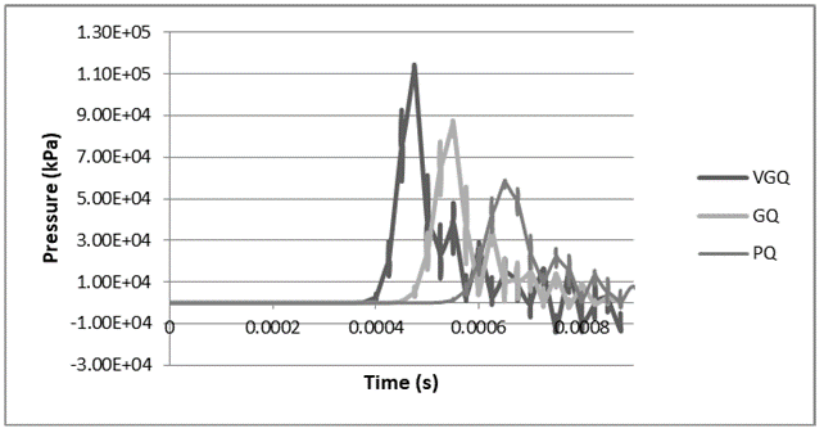

Fig. 9 Stress wave pressure variation over time, 2.00 m from the blast hole wall, for the three qualities of limestone

far from the blast hole. Pressure values are largely dependent on factors such as the nature and the density of the explosive material and the type of the rock mass, (Bhandari 1997). The stress wave attenuates over distance after the pressure fluctuation in the immediate vicinity of the blast hole.

This phenomenon is evident in Fig. 8, which presents the borehole pressure fluctuation at the wall of the blast hole, for the three types of limestone, as it was produced by the numerical model. The query point for the extraction of pressure value data is chosen to be a node at the wall of the blast hole, inside the model, in the middle of the arc. Specifically, the highest quality limestone (VGQ) displays the highest pressure of 1.55E+06 kPa, while the lowest

Table 3 P-wave velocities of stress wave for the three qualities of limestone, according to Eq. (5)

Limestone quality	P-wave velocity (m/s)
VGQ	4701
GQ	4038
PQ	3390

Table 4 Comparison of stress wave pressure arrival times between FEA model and theoretical calculation, 2.00 m away from the blast hole wall

	Pressure Wave Arrival Time(s)	
Limestone quality	**FEA Model**	**Theoretical Calculation**
VGQ	4.00E-04	4.25E-04
GQ	4.75E-04	4.95E-04
PQ	5.75E-04	5.89E-04

pressure of 1.27E+06 kPa corresponds to limestone with poor mechanical characteristics (PQ).

As far as pressure of stress wave build up and attenuation, inside the rock mass is concerned, it is expected that depending on the position of the measurement, there will be a delay of the pressure wave arrival with a gradual increase in pressure value and consecutive attenuation as the wave passes.

Fig. 9 depicts the fluctuation of the pressure of the stress wave at a node about 2.00 m away from the blast hole wall, in the middle of the model's thickness. As it can be seen, the very good quality limestone responds earlier to pressure, presenting a peak value of 1.13E+05 kPa, 4.75E-04 s after the event initiation. Comparatively, the pressure wave arrives later as the quality of limestone deteriorates and a delay in the forming of peak pressure of stress wave values is evident. Moreover, a gradual demise of the peak pressure value is observed from the very good to poor quality limestone.

The observed latency in the formation of peak pressure of stress wave values according to rock quality can be attributed to the P-wave velocity of stress wave, as it is expressed by Eq. (5), (Zhang 2016):

$$C_p = \sqrt{\frac{E(1-v)}{\rho(1+v)(1-2v)}} \tag{5}$$

where, C_p is the P-wave velocity of stress wave, E is the Young's modulus, v is the Poisson's ratio, and ρ is the density of the rock. The equation determines the propagation speed of a P-wave in the particular medium, according to its mechanical characteristics. It is evident that P-wave propagation depends on density as well as on other elastic constants of the rock. By implementing the equation for the three types of limestone, Table 3 is produced showing relevant resulting velocities. It is obvious that there is a gradual increase in P-wave velocity as the quality of limestone improves. Furthermore, Table 4 shows a comparison of stress wave pressure arrival times between the FEA model and simple theoretical calculation (constant velocity assumption). It is apparent that the difference is rather negligible and most likely without significant consequences for the validity of the numerical simulation.

3.2.1 Stress wave pressure attenuation over distance

Another important aspect of the phenomenon concerns the attenuation of stress waves inside the rock mass following the explosion, which is defined as the decrease in the amplitude as the propagation distance increases. The attenuation is mainly dependent on geometrical factors, material damage and fracture, internal friction and cracks of the material. The attenuation characteristics of the stress waves induced by rock blasting over distance, is expressed as a function of the peak pressure of stress waves on the wall of the explosive column and the distance from the explosive source. Specifically, the following equations, Eq. (6) and Eq. (7) describe the attenuation process (Li *et al.* 2011, Qiu *et al.* 2018):

$$P_r = P_d \left(\frac{d}{r}\right)^a \tag{6}$$

$$P_d = \frac{\rho_o D^2 2\rho C_p}{1 + \gamma\rho C_p + \rho_o D} \tag{7}$$

where, P_r is the peak pressure of stress waves at a distance r from the explosive source in the rock mass, P_d is the pressure on the rock face in the blast hole, d is the radius of the charge column and α is an attenuation coefficient (In the propagation area of a shock wave: $a = 2 + \frac{v}{1+v}$, in the propagation area of a stress wave: $a = 2 - \frac{v}{1+v}$). Furthermore v is the Poisson's ratio of the rock mass, ρ is the density of the rock mass, ρ_o is the density of the explosive, D is the detonation velocity of the explosive, γ is the adiabatic parameter of detonation products and C_p is the P-wave velocity of the rock mass.

Eqs. (6) and (7) were implemented using the geometric and mechanical characteristics of the present problem. A path ranging from the blast hole to a distance of 3.00 m away from the explosive source was chosen, in order to get a set of theoretical results. Accordingly, pressure values in relation to distance for the same path were also calculated by the FEA model. In Fig. 10 a representative diagram concerning the GQ limestone is presented. The resulting attenuation curves of peak pressure values over distance from both the theoretical and the FEA model are compared. In both cases and in accordance to theory, pressure of stress wave almost instantaneously maximizes and then attenuates along with distance from the explosive source. It is also observed that the attenuation curve of the FEA model generally coincides with the theoretical results. This further indicates the reliability of the numerical model in simulating the blast wave propagation inside the limestone, presenting successfully the attenuation properties of the rock during the blasting process.

3.3 Energy balance analysis

The evaluation of the energy balance in an explicit dynamic analysis is of great importance as it allows

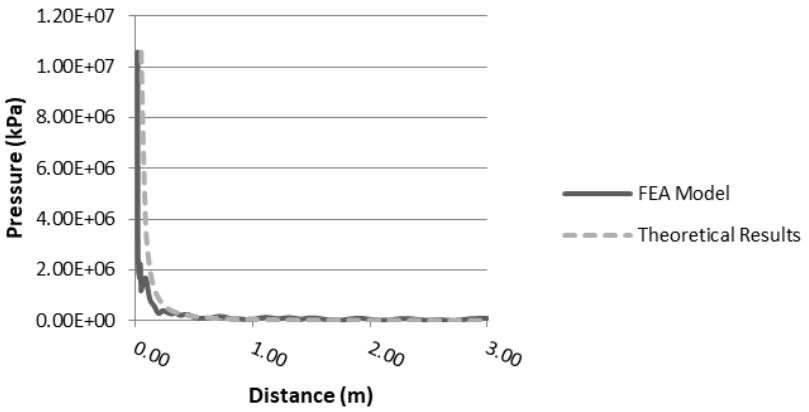

Fig. 10 Comparison of peak pressure attenuation curves between FEA model and theoretical results for limestone of good quality

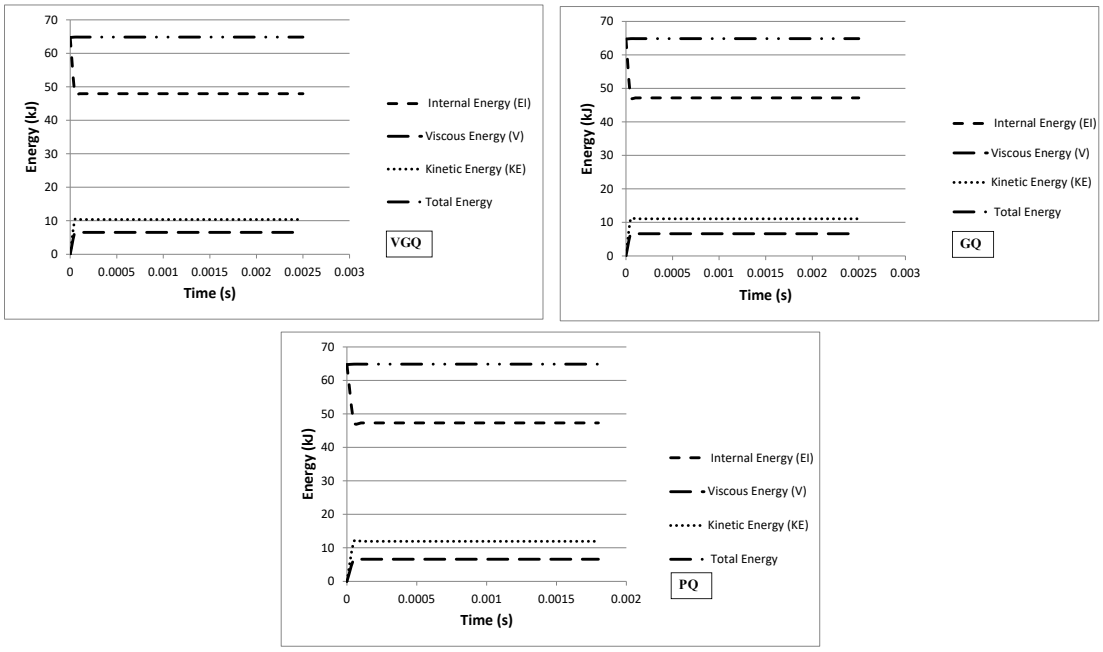

Fig. 11 The Total Energy and its components for the three types of simulated limestone

comparative analysis of various energy components that are developed after applying the explosive load in short time duration. The assessment of the energy quantities leads to the determination of the plausibility of the finite element model. In the process of simulating the blast event inside a rock mass, it is necessary to assess whether the model attributes in an appropriate way the dynamic transformation of the chemical energy to other forms of energy. Generally, the energy balance for the entire model is expressed as follows, Eq. (8) (Diehl 2012):

$$E_{total} = E_I + E_V + E_{FD} + E_{KE} + E_{IHE} - E_W - E_{PW} - E_{CW} - E_{MW} - E_{HF} \quad (8)$$

where, E_I is the Internal Energy, E_V is the Viscous Energy dissipated, E_{FD} is the Frictional Energy dissipated, E_{KE} is the Kinetic Energy, E_{IHE} is the Internal Heat Energy, E_W is the work done by the externally applied loads, E_{PW}, E_{CW}, E_{MW}, are the work done by contact penalties, by constraint penalties and by propelling added mass, respectively. E_{HF} is the External Heat Energy through external fluxes. The E_{total} value is the sum of the energy components and should be observed to present a constant value throughout the entire analysis, (Fig. 11).

Due to the nature of the present research and the corresponding analysis three energy components standout, such as the Internal Energy (E_I), the Viscous Energy (E_V) and the Kinetic Energy (E_{KE}). The internal energy is described by the following expression, Eq. (9):

$$E_I = E_E + E_P + E_{CD} + E_A + E_{DMD} + E_{DC} + E_{FC} \quad (9)$$

where the components are the recoverable Elastic Strain Energy (E_E), the Plastic Dissipated Energy (E_P), the Energy Dissipated through Viscoelasticity or creep (E_{CD}), the Artificial Strain Energy (E_A), the Energy Dissipated through Damage(E_{DMD}), the Energy Dissipated through Distortion Control (E_{DC}) and the Fluid Cavity Energy (E_{FC}).

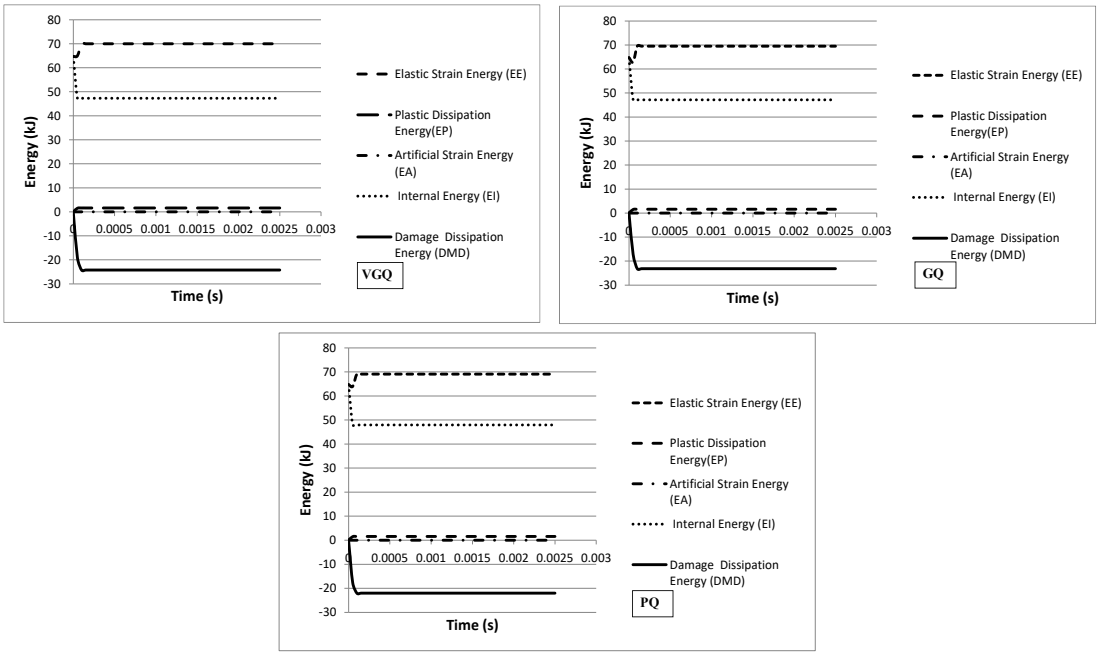

Fig. 12 The Internal Energy and its components for the three types of simulated limestone

The energy balance assessment for the three types of the simulated limestone is analyzed in the following paragraphs, resulting in conclusions that confirm the plausibility of the model.

Fig. 11 depicts the energy plots for the Total Energy and its components for the three types of simulated limestone, as they were calculated by the FEA model. An important component of the Total Energy is the Kinetic Energy (KE), as it is illustrated in the plot and it is delineated by an initial energy with a peak value of approximately 1.0E-04 s from the beginning of the explosion. In particular, it is noticed that the poor quality limestone presents the highest KE, allowing higher mobility of the particles due to the low density and stiffness of the material, while the lowest value of KE corresponds naturally to the limestone with better mechanical characteristics. The Total Energy is relatively constant throughout the three models presenting a value as high as 64.80 kJ, coinciding with the calculation by the geometrical characteristics of the blast hole and the ANFO properties (paragraph 2.3).

The Artificial Strain Energy, as a component of the Internal Energy, should and is found to be close to zero for all the FEA models with an average value of 3.14E-06 kJ, indicating the credibility of the FEA model as far as the accuracy of the meshing is concerned, (Fig. 12). According to sources from FEA related literature the Artificial Strain Energy should be less than 1-2% of the Internal Energy. In the simulated model for the three types of the limestone, the Artificial Strain Energy is estimated to be as low as 6.5 E-08% of the Internal Energy.

The simulated limestone presents an initial linear relationship between stress and strain, storing energy inside the rock before the elastic limit, indicating a recoverable Elastic Strain Energy (EE) of 4.36 kJ for the VGQ limestone, 4.79 kJ for the GQ and 5.28 kJ for the PQ. It is obvious that there is a reverse relationship between the quality of the limestone and the energy that is stored for the elastic response. The energy dissipated through the inelastic process - Plastic Dissipation Energy (EP), which succeeds the elastic behavior, is slightly higher for the PQ than the VGQ limestone.

As far as the energy dissipated through progressive damage, it is observed that the PQ limestone presents higher stiffness degradation, dissipating energy of 24 kJ than the VGQ limestone which presents a value of 22 kJ. As a result the Internal Energy (EI) output, which is the sum of the aforementioned variables, presents a general stable value for the three qualities of simulated limestone, but with a different distribution of the individual components.

According to the aforementioned, the limestone quality affects the energy balance presented by the FEA models, revealing in a plausible way the energy distribution during the blasting process inside the rock mass. The quality of the rock mass is strongly related to stiffness, plastic deformation potential, degradation evolution and failure point, affecting the overall elastic-plastic behavior, as well as the allocation of the various energy components.

4. Conclusions

The present study dealt with the investigation of the behavior of three types of limestone of varying quality under the typical blasting process used in quarries, in relation to time and space. The numerical method of Finite Element Analysis (FEA) was implemented, in order to simulate the blasting event on the pit face, examining in detail the conditions that are developed inside the rock mass.

The three types of limestone are designated as of Very Good Quality (VGQ), Good Quality (GQ) and Poor Quality (PQ), depending on their mechanical properties. The Finite

Element code was developed by applying the Jones-Wilkins-Lee (JWL) equation of state to describe the thermodynamic state of ANFO and the pressure dependent Drucker-Prager failure criterion in conjunction with a progressive damage model to define the limestone behavior under blasting induced high rate stress.

Various phenomena, such as stress wave propagation, borehole pressure development, pressure attenuation over distance and energy component analysis were examined throughout the duration of the simulation, giving answers about the rock mass response in the immediate vicinity and further away from the blast hole.

As far as stress propagation is concerned, a rapid increase in stress in combination with the destruction of the material in a local area around the explosive center was observed, by the numerical analysis. Smaller values of stress were observed as the wave was propagated radially away from the blast hole, indicating different stress distribution for the three types of limestone. Furthermore, a direct correlation between the quality of limestone and the wave propagation velocity is presented.

The borehole pressure was also investigated, specifying the peak pressure at the wall of the blast hole, for each type of limestone. A direct relationship between the quality of limestone and the evolution of borehole pressure over time was observed. Additionally, a significant varying amount of latency for the development of the peak pressure of the stress wave, in a specific distance from the blast hole, was observed, from the very good to poor quality of limestone. This is attributed to the P-wave velocity, which in turn depends on the density and other elastic constants of the rock mass. Moreover, a comparison between the numerical model and theoretical results concerning the attenuation properties of limestone indicated the reliability of the simulation, as the peak pressure attenuation curves over distance are broadly similar.

As far as the energy distribution during the blasting process is concerned, limestone quality strongly affected the energy balance, as it was presented by the FEA models. Therefore, it can be concluded that the stiffness as well as the plastic deformation potential, degradation evolution and failure point of each rock mass affected the allocation of the various energy components.

In conclusion, taking into account the aforementioned results, it is obvious that the FEA models provide extensive information about a complex and inaccessible phenomenon, giving great potential for further study and development. The current research has a prospect of development as far as additional characteristics of the limestone are concerned, such as the blastability of the rock mass, including various joint characteristics. It might be useful to delineate the various phenomena that are developed inside the rock mass with a more complex geometry, depending on the density, the length and the mechanical properties of pre-existed discontinuities. The numerical simulation of the rock mass fracturing is an attractive practice, which will give answers about the effect of the fracture topology on the blasting event.

Acknowledgments

This research is co-financed by Greece and the European Union (European Social Fund- ESF) through the Operational Programme «Human Resources Development, Education and Lifelong Learning» in the context of the project “Reinforcement of Postdoctoral Researchers - 2nd Cycle” (MIS-5033021), implemented by the State Scholarships Foundation (IKY).

References

Abbey, T. (2019), *Introduction to FEA-NAFEMS Training Course on Basic FEA*, NAFEMS Publications, Glasgow, U.K.

Alejano, L. and Bobet, A. (2012), “Drucker-Prager criterion”, *Rock Mech. Rock Eng.*, **45**, 995-999. https://doi.org/10.1007/s00603-012-0278-2.

Bhandari, S. (1997), *Engineering Rock Blasting Operations,* A.A. Balkema Publishers, Rotterdam, The Netherlands.

Christaras, B. (1996), “Non destructive methods for investigation of some mechanical properties of natural stones in the protection of monuments”, *B. Int. Assoc. Eng. Geol.*, **54**(1), 59-63. https://doi.org/10.1007/BF02600697.

Clark, B. (1987), *Principles of Rock Fragmentation*, John Wiley & Sons Inc., London, U.K.

Diehl, T. (2012), *Using Advanced Energy Methods to Enhance FEA And Experiments*, Smart Tools for Analysis -Bodie Technology Inc.

Dimitraki, L., Christaras, B., Marinos, V., Vlahavas, I. and Arampelos, N. (2019), “Predicting the average size of blasted rocks in aggregate quarries using artificial neural networks”, *B. Eng. Geol. Environ.*, **78**(4), 2717-2729. https://doi.org/10.1007/s10064-018-1270-1.

Dimitraki, L., Christaras, V., Marinos, V. and Chatziangelou, M. (2016), “The use of ultrasonic velocity for determining mechanical characteristics of limestones”, *Proceedings of the 15th Symposium Society of Geological Engineers and Technicians of Serbia*, Belgrade, Serbia, September.

Drucker, D.C. and Prager, W. (1952), “Soil mechanics and plastic analysis or limit design”, *Quart. Appl. Math.*, **10**(2), 157-165.

Franklin, A. and Maerz, H. (1989), “Photographic measurements of jointing and fragmentation”, *Int. J. Rock Mech. Min. Sci. Geomech. Abstr.*, **26**(6), 313. https://doi.org/10.1016/0148-9062(89)91642-2.

Golshani, A., Oda, M., Okui, Y., Takemura, T. and Munkhtogoo, E. (2007), “Numerical simulation of the excavation damaged zone around an opening in brittle rock”, *Int. J. Rock Mech. Min. Sci.*, **44**(6), 835-845. https://doi.org/10.1016/j.ijrmms.2006.12.005.

Hansson, H. (2009), “Determination of properties for emulsion explosives using cylinder expansion tests and numerical simulation”, Research Report No. 1, Department of Civil and Environmental Engineering-Division of Rock Engineering, Luleå University of Technology, Stockholm, Sweden.

Jaeger, J., Cook N. and Zimmerman R. (2007), *Fundamentals of Rock Mechanics*, (4th Edition), Wiley-Blackwell, New Jersey, U.S.A.

Kuznetsov, M. (1973), “The mean diameter of the fragments formed by blasting rock”, *Soviet Min.*, **9**, 144-148. https://doi.org/10.1007/BF02506177.

Kwon, S., Lee, C.S., Cho, S.J., Jeon, S.W. and Cho, W.J. (2009), “An investigation of the excavation damaged zone at the KAERI underground research tunnel”, *Tunn. Undergr. Sp. Tech.*, **24**(1), 1-13. https://doi.org/10.1016/j.tust.2008.01.004.

Li, H.B., Xia, X., Li, J. C., Zhao, J., Liu, B. and Liu, Y.Q. (2011), “Rock damage control in bedrock blasting excavation for a nuclear power plant”, *Int. J. Rock Mech. Min. Sci.*, **48**(2), 210-218. https://doi.org/10.1016/j.ijrmms.2010.11.016.

Li, W., An, X. and Li, H. (2018), “Limestone mechanical

deformation behavior and failure mechanisms: A review", *Acta Geochimica*, **37**(2), 153-170. https://doi.org/10.1007/s11631-017-0259-y.

Lilly, A. (1986), "Empirical method of assessing rock mass blastability", *Proceedings of the Large Open Pit Mining Conference*, Newman, California, U.S.A., October.

Liu, F., Silva, J., Yang S., Lv, H. and Zhang, J. (2019), "Influence of explosives distribution on coal fragmentation in top-coal caving mining", *Geomech. Eng.*, **18**(2), 111-119. http://doi.org/10.12989/gae.2019.18.2.111.

Ma, G. and An, X. (2008), "Numerical simulation of blasting-induced rock fractures", *International Int. J. Rock Mech. Min. Sci.*, **45**(6), 966-975. https://doi.org/10.1016/j.ijrmms.2007.12.002.

Menikoff, R. (2017), "JWL equation of state", Technical Report No.LA-UR-15-29536, Los Alamos National Lab. (LANL), Los Alamos, New Mexico, U.S.A.

Mohanty, B., (1996), *Rock Fragmentation by Blasting*, (1st Edition), CRC Press, Boca Raton, Florida, U.S.A.

Nie, L. and Olsson, M. (2000), "Study of mechanism by measuring pressure history in blast holes and crack lengths in rock", *Proceedings of the 27th Annual Conference on Explosives and Blasting Technique*, Orlando, Florida, U.S.A., January.

Ozacar, V. (2018), "New methodology to prevent blasting damages for shallow tunnel", *Geomech. Eng.*, **15**(6), 1227-1236. http://doi.org/10.12989/gae.2018.15.6.1227.

Potts, D. and Zdravkovic, l. (1999), *Finite Element Analysis in Geotechnical Engineering Theory*, Thomas Telford Publishing, London, U.K.

Qi, C., Wang, M., Bai, J., Wei, X. and Wang, H. (2016), "Investigation into size and strain rate effects on the strength of rock-like materials", *Int. J. Rock Mech. Min. Sci.*, **86**, 132-140. http://doi.org/10.1016/j.ijrmms.2016.04.008.

Qiu, X., Hao, Y., Shi, X., Hao H., Zhang, S. and Gou, Y. (2018), "Numerical simulation of stress wave interaction in short-delay blasting with a single free surface", *PLoS One*, **13**(9), e0204166. https://doi.org/10.1371/journal.pone.0204166.

Rosa, D. and Thornton, D. (2011), "Blast movement modeling and measurement", *Proceedings of the 35th Apcom Symposium,* Wollongong, Australia, September.

Rustan, A., Vutukur,i S., Naartijarvi, T. (1983), "The influence from specific charge, geometric scale and physical properties of homogenous rock on fragmentation", *Proceedings of the 1st International Symposium on Rock Fragmentation by Blasting*, Lulea, Sweden, August.

Sanchidrian, S., Castedo, R., Lopez, L., Segarra, P. and Santos, A. (2015), "Determination of the JWL constants for ANFO and emulsion explosives from cylinder test data", *Central Eur. J. Energ. Mater.*, **12**(2), 177-194.

Sazid, M. and Singh, T. (2012), "Two dimensional dynamic finite element simulation of rock blasting", *Arab. J. Geosci.*, **6**, 3703-3708. https://doi.org/10.1007/s12517-012-0632-4 .

Scott, A., Chitombo, P. and Kleine, T. (1993), "The challenge of the prediction and control of fragmentation in mining", *Proceedings of 4th International Symposium of Rock Fragmentation by Blasting*, Vienna, Austria, July.

Singh, P., Roy, M., Paswan, R., Sarim, M., Kumar, S. and Jha, R. (2016), "Rock fragmentation control in opencast blasting", *J. Rock Mech. Geotech. Eng.*, **6**(2), 225-237. https://doi.org/10.1016/j.jrmge.2015.10.005.

Song, Z., Li, S., Wang, J., Sun,Z., Liu, J. and Chang, Y. (2018), "Determination of equivalent blasting load considering millisecond delay effect", *Geomech. Eng.*, **15**(2), 745-754. https://doi.org/10.12989/gae.2018.15.2.745.

Souers, C., Wu. B. and Haselman, C. (1996), "Detonation equation of state at LLNL, 1995", Technical Report No. UCRL-ID-119262-Rev.3. Lawrence Livermore National Laboratory, Livermore, California, U.S.A.

Stagg, S., Otterness, E. and Siskind, E. (1992), "Effects of blasting practices on fragmentation", *Proceedings of the 33rd US Symposium in Rock Mechanics*, Santa Fe, New Mexico, June.

Stowe, R. (1969), "Strength and deformation properties of granite, basalt, limestone and tuff at various loading tests", Research Report No.69185, U.S. Army Engineer Waterways Experiment Station CORPS OF ENGINEERS, Vicksburg, Mississippi, U.S.A.

Wawersik, W. and Fairhurst, C. (1970), "A study of brittle rock fracture in laboratory compression experiments", *Int. J. Rock Mech. Min. Sci. Geomech. Abstr.*, **7**(5), 561-575. https://doi.org/10.1016/0148-9062(70)90007-0.

Yang, R., Bawden, W.F. and Katsabanis, P.D. (1996), "A new constitutive model for blast damage", *Int. J. Rock Mech. Min. Sci.*, **33**(8), 245-254. https://doi.org/10.1016/S0148-9062(97)87490-6.

Zhang, Y., Ding, X., Huang, S., Qin, Y., Li, P. and Li, Y. (2018), "Field measurement and numerical simulation of excavation damaged zone in a 2000 m-deep cavern", *Geomech. Eng.*, **16**(4), 399-413. https://doi.org/10.12989/gae.2018.16.4.399.

Zhang, Z.X. (2016), *Rock Fracture and Blasting, Theory and Applications*, Butterworth-Heinemann- Elsevier, Oxford, U.K.

Zhou, Z. (2010), "Numerical study of rock fracturing during blasting excavation", *Proceedings of the International Conference on Mechanic Automation and Control Engineering,* Wuhan, China, June.

CC